Investigating the Catalytic Activity of Sterile Alpha and TIR Motif Containing 1 (SARM1)

A Major Qualifying Project Report
Submitted to the Faculty of
Worcester Polytechnic Institute

In partial fulfillment of the requirements for the
Degree of Bachelor of Science by:

Eliza Mastergeorge
Biochemistry

Advised by:
Anita Mattson, Ph.D.
Department of Chemistry and Biochemistry, *WPI*

Paul R. Thompson, Ph.D.
Department of Biochemistry and Molecular Biotechnology, *UMass Chan Medical School*

ABSTRACT:

Wallerian degeneration of the axon is central to many neurodegenerative diseases and axonal injuries. The axon degeneration pathway involves two regulatory enzymes: nicotinamide mononucleotide adenylyltransferase 2 (NMNAT2) and sterile alpha and toll/interleukin receptor (TIR) motif-containing protein 1 (SARM1). Injury or disease causes a decrease in NMNAT2 levels, which leads to the activation of SARM1, a main contributor to axon degeneration. SARM1 catalyzes the hydrolysis of NAD+ to form nicotinamide (NAM), ADP ribose (ADPR), and cyclic ADPR (cADPR) in the NAD+ salvage pathway, but little is still known about the mechanism by which this catalysis happens. This study indicates that there may be another cellular component necessary for ADP ribosylation catalysis by SARM1. Additionally, mutations to the active site showed increased catalytic efficiency and ADP ribosylation, further indicating a link between this site and SARM1's activity. Future studies on the effect of various mutations on the activity of SARM1 in different metabolite concentrations will help further the understanding of the mechanism and conditions by which SARM1 catalyzes NAD+ hydrolysis.

ACKNOWLEDGEMENTS:

First, I would like to thank Professor Anita Mattson (WPI) for helping me navigate the challenges of working independently on an off-campus project, I am extremely grateful for her advice and support. Thank you also to Professor Paul R. Thompson (UMass) for giving me the opportunity to gain hands-on experience in his lab and for walking through experimental design and results with me so that I could fully understand the concepts. Thank you to everyone working in the Thompson Lab who was always willing to help me find what I was looking for and answer my questions. Thank you especially to Janneke Doedee Isco for teaching me so many lab skills and concepts, supplying me with protein when my purifications wouldn't work, and guiding me throughout this experience. Finally, thank you to all of my friends, family, and classmates who have been by my side encouraging me throughout my entire academic journey.

TABLE OF CONTENTS:

INTRODUCTION AND BACKGROUND:

Wallerian Degeneration:

Wallerian degeneration, first described in 1850 by neurologist Augustus Waller, is the process that occurs when transportation is disrupted in the axon of a neuron, causing a decrease of nicotinamide nucleotide adenylyltransferase 2 (NMNAT2) which eventually leads to the degeneration of the axon itself (1). Initial studies observed this phenomenon as a result of physical injury in which the axon was severed entirely, cutting off all delivery to the axon, as can be seen in Figure 1. The loss of NMNAT2 activates sterile alpha and TIR motif containing 1 (SARM1), an enzyme that catalyzes the processes that contribute to the degeneration of the axon (2).

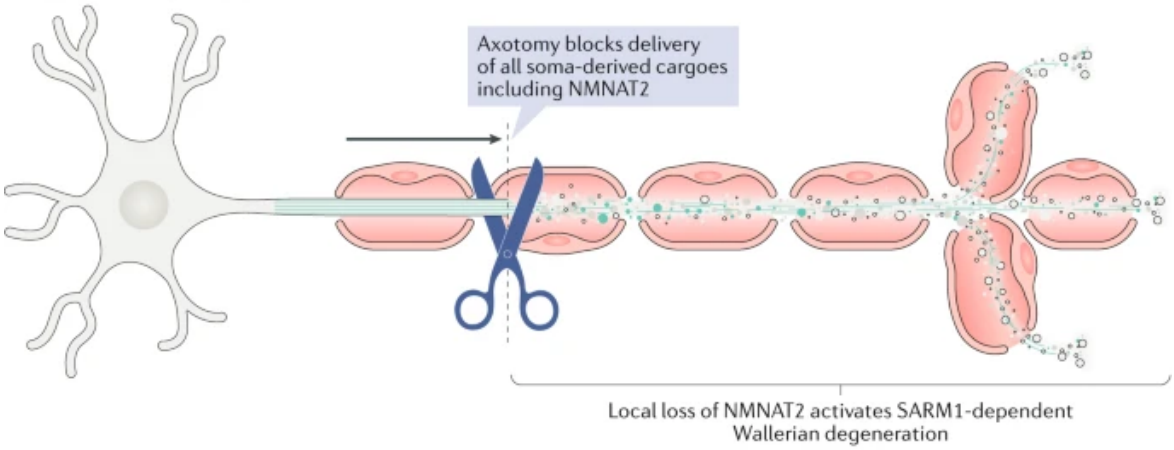

Figure 1. Activation of Wallerian degeneration resulting from injury (2)

Recent studies have shown that the same degeneration pathway is involved in a number of human diseases, such as Alzheimer's disease, peripheral neuropathy, and amyotrophic lateral

sclerosis (ALS) (2). Rather than a severed axon blocking cargo delivery, the transport is impaired due to the disease, resulting in the activation of SARM1. This process is illustrated in Figure 2.

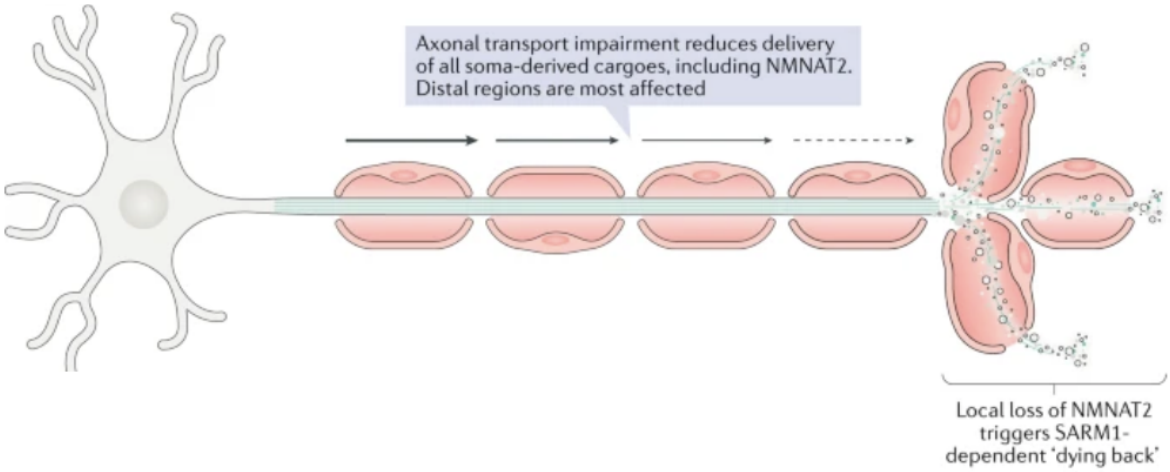

Figure 2. Activation of Wallerian degeneration resulting from disease (2)

Axon degeneration occurs in three phases: initiation, latency, and execution. The initiation phase occurs briefly after the axotomy occurs and lasts for around 12 hours. During this time, it is still possible to delay degeneration (3). The latency phase occurs up to 24 hours after injury (4). In this stage, the reduced delivery of NMNAT2 causes a shift in which the NAD^+ levels decrease while NMN levels rise. This shift in the NAD^+/NMN ratio leads to the activation of SARM1. Finally, the execution phase is the final stage of Wallerian degeneration, which occurs after up to 36 hours after injury. The influx of Ca^{2+} resulting from the production of (c)ADPR by SARM1 activates calpain, which is a protease that cleaves spectrin and tubulin, components of microtubules that are vital to axon structure (5).

NAD^+ Metabolism in the Axon Degeneration Pathway

In a healthy neuron, NMNAT2 converts NMN to NAD^+, helping maintain NAD^+ stores in the body as a part of the NAD^+ salvage pathway. SARM1 is kept inactivated by NAD^+ by binding to the allosteric site; so when NAD^+ levels are reduced and NMN levels are increased, a conformational change is initated as NMN outcompetes NAD^+ for binding. This change leads to the activaton of SARM1 activity, and it begins to catalyze the hydrolysis of NAD^+ to Nicotinamide and (c)ADPR (7).

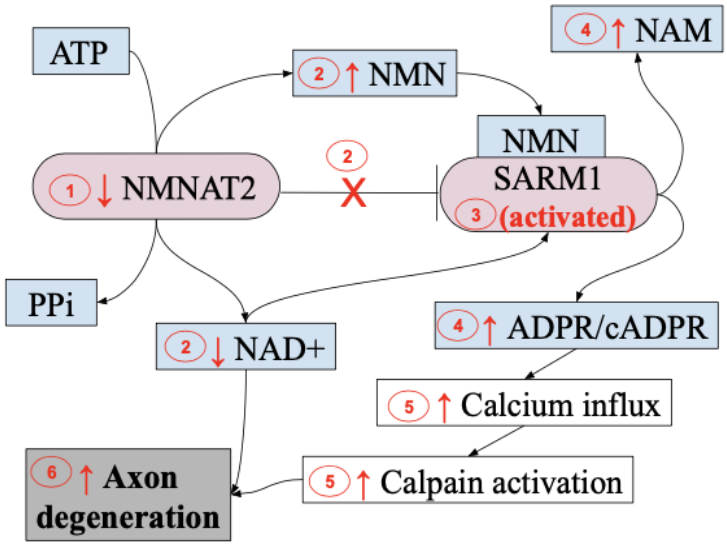

Figure 3. Wallerian degeneration metabolic pathway

1. Injury or disease reduces axonal delivery of NMNAT2. 2. NAD^+ levels decrease and NMN levels increase; NMNAT2 no longer inhibits SARM1. 3. NMN activates SARM1, combined with reduced NAD^+ levels to drive catalysis forward. 4. SARM1 catalyzes the production of Nicotinamide and (c)ADPR; the increase in (c)ADPR levels induces a calcium influx, which activates calpain. 6. Decreased NAD^+ levels and calpain activation contribute to the degeneration of the axon.

SARM1 Structure and Binding:

SARM1 is a ring-shaped octamer composed of four regions: the N-terminal peptide is responsible for mediating mitochondrial targeting; the ARM-repeats region regulates autoinhibition; the two SAM domains manage the molecule's oligomerization, and the TIR domain is responsible for the enzyme's NADase activity (6).

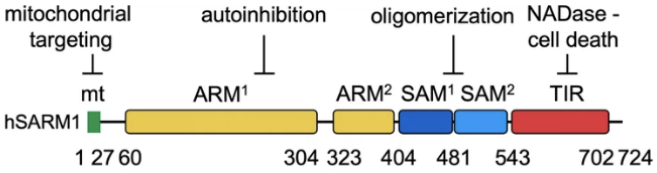

Figure 4. Organization of the hSARM1 domains and their targets (6)

The ARM regions are responsible for blocking activity in the TIR domain when in homeostatic conditions. The "BB" loop of the TIR domain flips inward to meet with the "EE" loop of another TIR domain, obstructing NAD^+ entry into the TIR domain substrate pocket (6). NAD^+ instead binds allosterically to the ARM domain via a number of electrostatic interactions which are thought to contribute to SARM1 inhibition. NMN competes with NAD^+ for binding this site. When NMN is bound instead of NAD^+, the ARM domain interferes with the TIR domain, which encourages SARM1 to assemble into its active conformation. This is why the NMN/NAD^+ ratio is crucial for maintaining SARM1 inactivation (9).

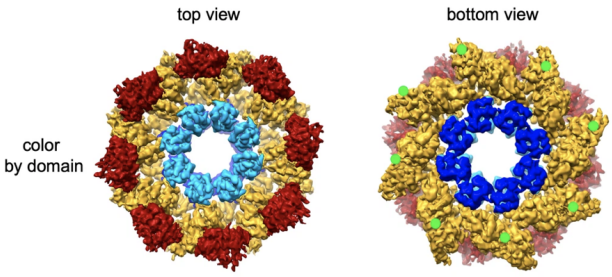

Figure 5. Cryo-EM density map of hSARM1 (6)

Domain colors coordinate with labels in Figure 4

hSARM1 Mutations of Interest

hSARM1$^{\Delta MLS}$

This is the version of SARM1 used for the wild type SARM1 model. It is a slightly truncated sequence with the mitochondrial targeting domain removed (9).

hSARM1^{E642A}

E642 is located in the TIR domain's active site and is involved in. Therefore, substitutions at this site abolish NADase activity and render SARM1 catalytically inactive (9).

hSARM1^{H685A} and hSARM1^{G601P}

H685 and G601 are located in the EE and BB loops of the TIR domain which contribute to the blocking of the active site. Substitutions here would affect the oligomerization of the molecule and would be expected to increase activity (9).

METHODS AND PROCEDURES:

SARM1$^{\Delta MLS}$ and SARM1^{E642A} Purification:

Polymerase Chain Reaction (PCR) Amplification

The Bio-Rad iProof™ High-Fidelity PCR kit was used to amplify the SARM1$^{\Delta MLS}$ and SARM1^{E642A} sequences for purification. The reaction conditions used were those of a typical reaction setup per manufacturer's protocols, with the exception of GC buffer being used instead of HF buffer. The final concentrations were 1X iProof GC buffer, 200µM dNTP mix, 0.5µM of each primer, 50ng DNA template, 0.02U/µL iProof DNA Polymerase, and sterile water to total 50µL.

Once the components were combined, the samples were denatured at 98°C for 30 seconds before entering a denaturation/annealing/extension cycle for 30 repetitions. The denaturation step was conducted at 98°C for 10 seconds, the annealing step at the specified temperature condition (i.e. Tm-5) for 30 seconds, and the extension step at 72° for 2 minutes. Then, a final extension was initiated at 72° for 10 minutes, until the cycler temperature was held at 4°C until the samples were removed.

Bacterial Transformation and Plasmid Purification

Once the DNA sequence was amplified by PCR, it was transformed into XL1-Blue competent cells. For generating the mutant SARM1^{E642A}, 2µL DpnI was added to 50µL PCR reactions and incubated at 37°C for 2 hours before the transformation was initiated. 10µL DNA from the PCR reactions was added to 100µL thawed competent cells and the tubes were left on ice for 30 minutes before being heat shocked for 45 seconds in a heat block at 42°C. The cells

were then recovered for 5 minutes on ice before 1mL LB media was added to each tube. The tubes were incubated on a rotator for a minimum of one hour at 37°C; LB agar plates treated with ampicillin and tetracycline were also warmed in the 37°C incubator during this time. After incubation, the cultures were spun for 1 minute at 5000 x g, the supernatant was poured off, and the pellet was resuspended in the remaining liquid. The resuspension was pipetted onto the prewarmed media plates and spread using a sterilized spreader. The plates were incubated overnight at 37°C and colonies were picked the following day or the plates were stored at 4°C until the colonies were picked.

Sterile culture tubes were prepared with 8mL LB media, 100µg/mL ampicillin, and 10µg/mL tetracycline. One colony was selected from each PCR preparation using a pipette tip, and the pipette tip was ejected into the prepared reaction tubes, which were incubated overnight in the rotator at 37°C to allow for further growth of the selected colony. The next day, the samples were concentrated in a centrifuge and the supernatant was poured off leaving plasmid DNA. This plasmid DNA was purified using the QIAGEN Midi/Maxi Plasmid Kits following the manufacturer's protocols. The amount of DNA present in each sample was quantified using a ThermoFisher NanoDrop Spectrophotometer, and concentrations of 80ng/µL were prepared. 10µL of this DNA was combined with 5µL of the designated primer(s) near the protein of interest and the sample was sent out for Sanger Sequencing through GENEWIZ.

Protein Transfection

The day prior to transfection, Expi293F cells were grown in FreeStyle Expression Medium, passaged once they reached a density of 2.5 x 10^6 viable cells/mL, and then incubated overnight at 33°C. FreeStyle expression medium and Opti-MEM were pre-warmed in a 37°C

water bath while the DNA was prepared. 90µg DNA was diluted in 1.5mL Opti-MEM and allowed to incubate for five minutes to achieve a final concentration of 60µg DNA/mL. A solution of polyethyleneimine (PEI) was prepared in 25mM HEPES, pH 7.5, and 150mM NaCl to a concentration of 1mg/mL; the solution was vortexed until the PEI was fully dissolved, and the solution was filter-sterilized. Then, the PEI and DNA were combined and incubated for 30 minutes at room temperature. After this, the cells were diluted to 2.5 x 10^6 cells/mL by spinning down the required amount of cells and resuspending them in 27mL of fresh media. 3mL of the PEI-DNA mixture was added to the cells, and the cultures were returned to the incubator overnight. The next day, 29.2mg of valproic acid was dissolved in 40mL FreeStyle Medium and filter sterilized. An equivalent volume of valproic acid was added to dilute the cells 1:1, and they were harvested by centrifugation after incubating for 3 more days at 33°C. Harvested cells were flash-frozen and held at -80°C.

Protein Purification

The initial stages of protein purification were the same for both wild type and E642A purifications, but the final method of protein elution varied slightly. ~200µL samples were taken of each step of purification and each resin for analysis by SDS-PAGE. For both procedures, the pellets of harvested cells were thawed on ice and resuspended in 2mL Lysis buffer containing 50mM HEPES, pH 8; 400mM NaCl; and 5% glycerol (w/v), along with Pierce™ protease inhibitor mini tablets. The resuspension was sonicated in 5mL batches in a series of 10 sonications with an amplitude of 10, a 10-second processing time, 1s on and 1s off, and a 20s delay between cycles. This lysate was clarified by centrifugation at 15,000 x g at 4°C for 10 min. Meanwhile, 1mL CBV IgG agarose was equilibrated with lysis buffer in a column. The clarified

lysate supernatant was poured onto the column and bound for 1 hour at 4°C on an end-over-end rocker. The column was then opened to allow for flow by gravity before being washed with 10 CV of lysis buffer, followed by 5 CV wash 2, which is composed of 25mM HEPES, pH 7.4, and 150 mM NaCl.

For wild type purification, 40µL PreScission Protease was mixed with 960µL wash 2. The resin was resuspended with this mixture and incubated overnight at 4°C without rocking. The next day, the column was opened to allow for flow by gravity, then washed with 5 CV wash 2, twice in series. 1mL CBV Glutathione Sepharose (GST) was equilibrated with wash 2 in a new column. The eluate from the day 2 gravity flow and first wash were added to the column with a stopper and allowed to bind for 30 minutes. The column was opened, the eluate was collected, and the resin was washed twice with 5 CV wash 2.

For E642A purification, rather than binding with another resin, the protein was eluted from the IgG agarose column with 5 CV elution buffer containing 100mM glycine, pH 2.5-3. The elutions were collected in 3mL fractions and each fraction was neutralized with 300µL neutralization buffer, which contains 1 M HEPES, pH 7.4. Fractions containing pure protein as determiuned by SDS-PAGE were combined and poured into 12-14kD RC tubing to undergo dialysis overnight in 4L of buffer containing 1M HEPES and 5M NaCl. The precipitates were spun out of the dialized protein and it was concentrated in a centrifuge.

SDS-PAGE and Protein Quantification

Samples of each stage of purification were collected to use for SDS-PAGE analysis to assess the purity at each stage. Fractions were taken of the lysate, clarified lysate, cell resuspension, resins, and every elution. 40µL of each sample was combined with 10µL 5X SDS

and incubated at 95°C for 10 minutes. 10µL of each sample was loaded onto a 4-20% Mini-PROTEAN® TGX Stain-Free™ gel, with 1X PBS as a running buffer. A current was run at 150-170V until the dye front reached the bottom of the gel. A stain-free scan was taken, and then the gel was stained with Coomassie-Blue stain and a scan was taken on a white plate.

The pure proteins and lysates were quantified by Bio-Rad protein assay and Bio-Rad DC assay respectively. The protocol was followed according to manufacturer's instructions with the exception that incubation time required 30-45 minutes, as opposed to the 5 minutes recommended. The absorbance of the protein and lysate mixed with different reagents was compared to the absorbance of a BSA standard curve mixed with the same reagents to determine the concentration of protein in the purified protein and lysate samples.

Generation of Additional Mutants:

Identifying Primers

Forward and reverse primers were designed for both mutants being generated. First, the amino acid position number was multiplied by three to identify the nucleotide. The codon of interest was identified and ~15 codons before and after were isolated. The specific amino acid necessary for the required mutation could now be swapped in.

In selecting the section of the sequence for the primer, it was important to aim for 40-60% G:C content while also ending with a G or C (ideally two in a row). The nucleotide at the 3' end was the same as the 5' end and secondary structurers were avoided. A sequence length of 28-36 nucleotides was selected for the forward primer. The reverse complement of the forward primer was used to generate a reverse primer. This was done for H685A and G601P.

PCR Conditions Tested

Once the primers were selected, multiple attempts were made to conduct a PCR, testing various conditions. The first conditions attempted were using the Bio-Rad iProof™ High-Fidelity PCR Kit. The conditions utilized followed the manufacturer's recommendations of a typical reaction setup with 50µL total containing 1X iProof™ GC buffer, 200µM dNTP mix, 0.5µM of each primer, a select amount of DNA, and 0.02 U/µL iProof™ DNA Polymerase. Conditions were tested with 10 and 50ng of DNA template at Tm-5, Tm-3, and Tm+3. Various conditions were attempted, involving HF buffer instead of GC buffer, adding 3% Dimethyl Sulfoxide (DMSO), and switching the polymerase. Finally, the last condition tested used the NEBNext® High-Fidelity 2X Master Kit which only requires the addition of 0.5µM of each primer and the select amounts of DNA: 10 and 50ng. This was also tested in +/- 3% DMSO at Tm-5, Tm-3, Tm, and Tm+3.

The cycling conditions used were the same for each condition tested. The samples were denatured at 98°C for 30 seconds before entering a denaturation/annealing/extension cycle for 30 repetitions. The denaturation step was conducted at 98°C for 10 seconds, the annealing step at the specified temperature condition (i.e. Tm-5) for 30 seconds, and the extension step at 72° for 2 minutes. Then, a final extension was initiated at 72° for 10 minutes, before the cycler temperature was held at 4°C until the samples were removed.

The DNA was transformed into XL1-Blue competent cells, spun down, and the plasmid was purified with a QIAGEN Mini Prep Kit, similar to the protocol above for wild type and E642A SARM1. The amount of DNA present in each sample was quantified using a ThermoFisher NanoDrop Spectrophotometer, and concentrations of 80ng/µL were prepared. 10µL of this DNA was combined with 5µL of the designated primer(s) near the protein of

interest and the sample was sent out for Sanger Sequencing through GENEWIZ to determine whether the mutation was successful.

ADP Ribosylation Activity Western Blot Assay:

The ADP ribosylation activity of WT and E642A Lysate and Protein were compared in the presence and absence of NAD^+. Each sample was prepared in duplicate so they could all be tested for both their mono- and poly- ADP Ribosylation activity. 20µg of lysate or 500ng of protein was used per well. 48µL samples were prepared of each lysate/protein, +/- 1mM NAD^+, and 1X assay buffer composed of 250mM HEPES, pH 7.5 and 1.5M NaCl. The samples were incubated at room temperature for 30 minutes before adding 12µL 5X SDS and heating samples to 95°C for 10 minutes. 10µL of each sample was loaded onto a 4-20% Mini-PROTEAN® TGX Stain-Free™ gel, with 1X PBS as a running buffer. The gel was run at 125-150V until all of the dye had run off the gel, at which point a stain free image was captured.

Meanwhile, the transfer was prepared. 150mL 10X Western buffer and 300mL methanol were combined and water was added to a total of 1.5L. The membrane and filters were cut to the size of the gel and the membrane was activated in methanol for 1-2 minutes before it was poured off rinsed with the transfer buffer. The various components involved were left to soak in the buffer while the initial gel was being run. Then a sandwich was prepared with the cartridge, pads, filter papers, gel, and activated membrane, rolling gently between layers and keeping all of the materials wet. The cartridge was closed and placed in the chamber, which was filled with transfer buffer, along with an ice pack; the transfer was run at 80V for 1 hour.

Once the transfer was complete, the membrane was blocked in 5% BSA in 1X PBST for 15 minutes to an hour. Then, the primary antibody was added, and the membrane was incubated

for one hour at room temperature. For monoribosylation, anti mono ADP ribose was added in a concentration of 1:250; for polyribosylation, anti poly ADP ribose was added at a concentration of 1:1000. Once this incubation period was up, the membranes were briefly washed in PBST. Then, the membranes were rocked at room temperature for one hour in 5% BSA in 1X PBST containing the secondary antibody. For monoribosylation this was an anti-rabbit antibody, which was used at a ratio of 1:8000; and for polyribosylation, this was an anti-mouse antibody, used at a ratio of 1:5000. After this incubation, the membranes were washed three times in 1X PBST for 10 minutes each and then twice in water for five minutes each. Finally the membranes were scanned for analysis.

Enzyme Activity Kinetic Assay:

An enzyme kinetic assay was performed on the purified proteins to analyze the catalytic activity of wild type and E642A SARM1. Eight concentrations of ENAD were prepared by serial dilution ranging from 1000μM to 0. On a black microassay plate, 0.75μM of enzyme, 6μL 10X Assay Buffer, and water was combined to total 57μL. The wells were mixed at room temperature and the PerkinElmer® EnVision® plate reader was set up to record the fluorescence of each well every 15 seconds over the course of 20 minutes. The ENAD dilutions were added, the samples quickly mixed, and the plate was inserted into the reader. A standard curve was generated similarly, using cADPR cyclase to calculate the concentration of protein and the reaction velocity of each purification as well as determine the kinetic parameters.

RESULTS AND DISCUSSION:

Purification of SARM1$^{\Delta MLS}$ and SARM1^{E642A}:

Initial attempts at purifying wild type protein were unsuccessful at various stages. After analyzing the gels, the second wash buffer was remade and the IgG flowthrough was allowed to bind to the GST column for 30 minutes as opposed to being flowed through the column as was initially indicated in the protocol. These adjustments resulted in a successfully purified protein sample, the gel of which can be seen in Figure 6. The purified protein band can be seen at 77kDa, and the pure protein sample appears in the GST flowthrough. A protein assay was performed per manufacturer's protocols with BSA used for the standard curve. The final concentration of this purification was 0.825mg/mL and the total yield was 495µg of purified protein.

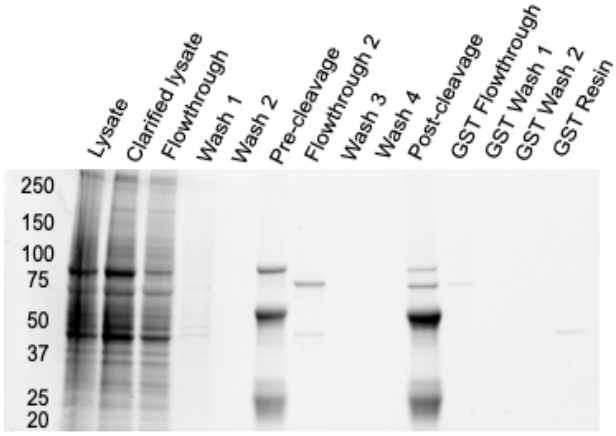

Figure 6. Unstained SDS-PAGE gel of samples from SARM1$^{\Delta MLS}$ purification

The E642A mutant purification was successful from the first attempt, with one example gel shown in Figure 7. Again, the purified protein band can be seen at 77kDa; here it is present in

Elutions 1 and 2, which were then combined. A protein assay showed the final concentration of this purification to be 1.008mg/mL and the final yield was 500µg of purified protein.

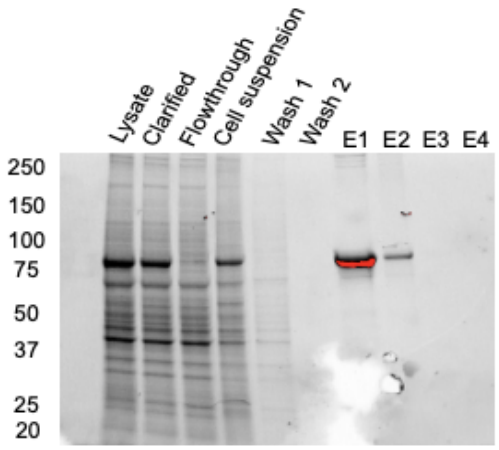

Figure 7. Unstained SDS-PAGE gel of samples from SARM1^{E642A} purification

G601P and H685A Mutant Generation:

The first PCR condition tested was performed on both G601P and H685A. Conditions included: 10 or 50ng DNA; temperatures: Tm-5, Tm-3, and Tm+3; GC Buffer; and BioRad iProof™ High-Fidelity DNA Polymerase. The Sanger sequencing returned for these conditions did not show the desired mutations, so the same conditions were tested again with the exception of HF Buffer substituting the GC Buffer and samples were tested in both the presence and absence of 3% DMSO. After this sequencing also showed no success in mutating the DNA, a new DNA polymerase was used.

In order to easily test more conditions, the decision was made to prioritize one mutant over the other, so the following attempts were only conducted on H685A. The same DNA concentrations and temperature conditions were tested in GC Buffer using the Phusion High-Fidelity DNA Polymerase in the presence and absence of DMSO. Again, these conditions

proved unsuccessful. Finally, rather than using a buffer and polymerase, the NEBNext® High-Fidelity 2X PCR Master Kit was used. The same DNA concentrations and temperature conditions were tested, with the addition of one more temperature: Tm of the primer. This was also tested in the presence and absence of DMSO. Successful mutations were identified by Sanger sequencing in a number of conditions which can be seen in Table 1.

DNA (ng)	Temperature	DMSO
10	Tm	+
50	Tm	+/-
10	Tm-3	-
50	Tm-3	+/-
50	Tm-5	+

Table 1. Successful PCR conditions for the mutation of SARM1^{H685A}

ADP Ribosylation in E642A and WT:

The Western Blot assay from the ADP Ribosylation experiment can be seen below in Figure 8. Untransfected lysate and wild type protein don't appear to undergo any ADP ribosylation. Ribosylation occurs much more in E642A lysate than in wild type lysate. Samples with NAD present showed slightly more ribosylation.

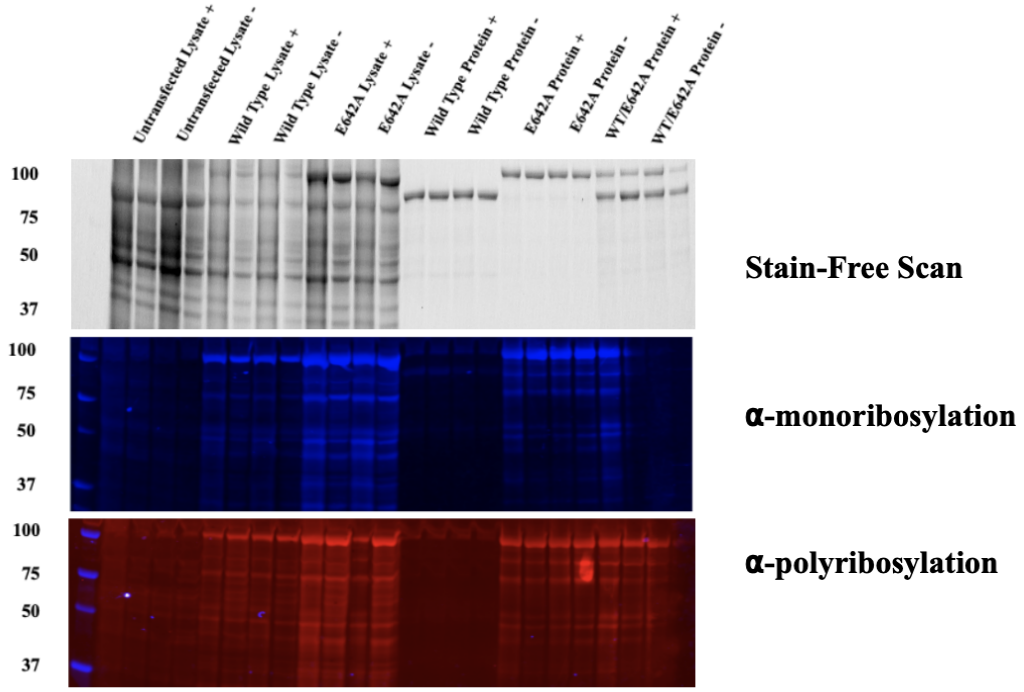

Figure 8. Stain-Free and Western blot scans of SARM1$^{\Delta MLS}$ and SARM1^{E642A} lysates and purified proteins in the presence and absence of NAD^{+}

Catalytic Efficiency of E642A and WT:

The measured absorbance values were recorded and compared to the standard curve generated in order to determine the amount of product generated at each time point. The slope of that amount of product generated over time was used to calculate the reaction velocity, which was used to generate a Michaelis-Menten curve, as seen in Figure 9. The software used to generate this curve, Prism, automatically provided the Km and Kcat, which were used to calculate the catalytic efficiency (Kcat/Km); all of which can be found in Table 2. The wild type protein has a much higher Km, indicating that the rate of product formation is more dependent on substrate concentration for wild type than the E642A mutant. The catalytic rate of the wild

type protein is around double that of the E642A mutant, and the catalytic efficiency of wild type protein is about 60% that of E642A.

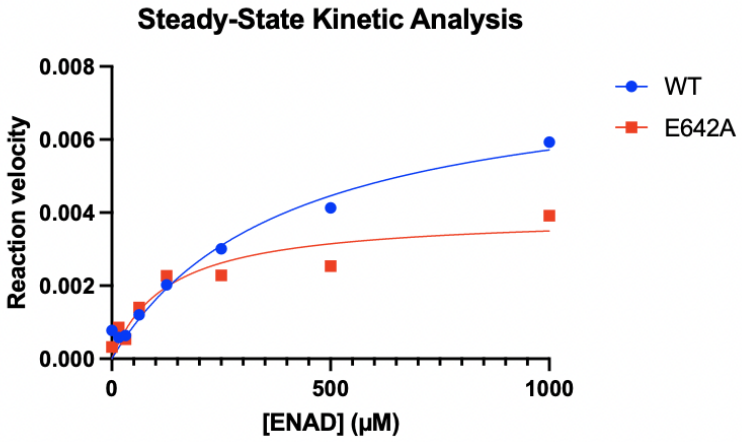

Figure 9. Michaelis-Menten curves for SARM1$^{\Delta MLS}$ and SARM1^{E642A} Fluorescent Assays

	WT	**E642A**
Km (µM)	390	126
Kcat (s^{-1})	0.0106	0.00525
Kcat/Km ($M^{-1}s^{-1}$)	27.0	41.8

Table 2. Calculated kinetic parameters for SARM1$^{\Delta MLS}$ and SARM1^{E642A}

CONCLUSIONS AND FUTURE DIRECTIONS:

Through multiple attempts, both wild type and E642A SARM1 protein were successfully purified. Improvements were made to the protocol as information was gathered from successful and unsuccessful purification attempts. One improvement made to the wild type purification protocol was to ensure that the eluates from the IgG column were allowed to bind to the GST column for at least 30 minutes before proceeding. The first E642A protein purification was separated by high performance lipid chromatography (HPLC), and a DC assay was performed to determine the protein concentration. This method of isolating the protein did not prove any more effective than the dialysis step at separating the protein from other substances, so HPLC was not conducted on remaining purifications.

SARM1^{H685A} DNA was successfully generated by PCR after various unsuccessful attempts. This protocol should be used in attempts at generating SARM1^{G601P} and other mutations that could provide insight into the binding mechanisms of SARM1. The recommended conditions are 50ng DNA with the NEBNext® Master Mix and 3% DMSO at temperatures: Tm, Tm-3, and Tm-5. Now that a PCR protocol has been established, SARM1^{H685A} protein can be isolated and used to gain more insight into how SARM1 is oligomerized.

The lack of ADP ribosylation in wild type protein despite it's presence in lysate was an unexpected occurrence that may indicate that there is an important cellular component necessary for ribosylation that is removed in the purification process. Further studies, including a Western Blot comparing SARM1 and BSA ADP ribosylation activity have been proposed to help learn more about why this could be occurring. The E642A mutants and lysates showed greater ADP ribosylation than the wild type; and ribosylation was slightly increased in the samples with NAD+ present. This was the opposite effect as was expected, as previous reports have noted that

E642A mutations abolish NADase activity in vitro, but the increased ribosylation displays increased activity. However, this does still indicate a link between E642 and the NADase activity of SARM1.

Similarly, the kinetic assays of E642A showed greater catalytic efficiency than wild type. Again, this was the opposite of the expected effect, but coincides with the results from the Western Blots. More studies with different substitutions at the E642 site or testing different substrate and metabolite concentrations would help provide more insight as to why this mutation appeared to increase activity rather than decrease it.

REFERENCES:

1. Waller, A. Experiments on the section of the glossopharyngeal and hypoglossal nerves of the frog, and observations of the alterations produced thereby in the structure of their primitive fibres. (1850). *Philos. Trans. R. Soc. Lond.* 140, 423–429.
2. Coleman, M.P., Höke, A. (2020). Programmed axon degeneration: from mouse to mechanism to medicine. *Nat Rev Neurosci,* 21, 183–196. https://doi.org/10.1038/s41583-020-0269-3
3. Loring HS, Thompson PR. Emergence of SARM1 as a Potential Therapeutic Target for Wallerian-type Diseases. (2020). Cell Chem Biol. 27(1):1-13. doi:10.1016/j.chembiol.2019.11.002
4. Jiang, Y., Liu, T., Lee, CH. *et al.* The NAD+-mediated self-inhibition mechanism of pro-neurodegenerative SARM1. (2020) *Nature,* 588, 658–663. https://doi.org/10.1038/s41586-020-2862-z
5. Hopkins, E. L., Gu, W., Kobe, B., & Coleman, M. P.A Novel NAD Signaling Mechanism in Axon Degeneration and its Relationship to Innate Immunity. (2021). *Frontiers in Molecular Biosciences*, *8*. https://doi.org/10.3389/fmolb.2021.703532
6. Sporny, M., Guez-Haddad, J., Khazma, T., Yaron, A., Dessau, M., Shkolnisky, Y., Mim, C., Isupov, M. N., Zalk, R., Hons, M., & Opatowsky, Y. Structural basis for SARM1 inhibition and activation under energetic stress. (2020). *eLife*, *9*, e62021. https://doi.org/10.7554/eLife.62021
7. Navarro, M. N., Gómez de Las Heras, M. M., & Mittelbrunn, M. Nicotinamide adenine dinucleotide metabolism in the immune response, autoimmunity and inflammageing.

(2022). *British journal of pharmacology*, *179*(9), 1839–1856. https://doi.org/10.1111/bph.15477

8. Wang, J. T., Medress, Z. A., & Barres, B. A. Axon degeneration: molecular mechanisms of a self-destruction pathway. (2012). *The Journal of cell biology*, *196*(1), 7–18. https://doi.org/10.1083/jcb.201108111
9. Wang, J., & He, Z.NAD and axon degeneration: from the Wlds gene to neurochemistry. (2009). *Cell adhesion & migration*, *3*(1), 77–87. https://doi.org/10.4161/cam.3.1.7483
10. Icso, J.D., Thompson, P.R. The chemical biology of NAD+ regulation in axon degeneration. (2022). *Current Opinion in Chemical Biology,* 69, 102176, ISSN 1367-5931, https://doi.org/10.1016/j.cbpa.2022.102176.